

OPEN

An inhibitor of apoptosis protein (*EslAP1*) from Chinese mitten crab *Eriocheir sinensis* regulates apoptosis through inhibiting the activity of *EsCaspase-3/7-1*

Chen Qu¹, Jiejie Sun¹, Qingsong Xu^{1,4}, Xiaojing Lv^{1,2,3,4}, Wen Yang¹, Feifei Wang¹, Ying Wang¹, Qilin Yi^{1,3,4}, Zhihao Jia², Lingling Wang^{1,2,3,4} & Linsheng Song^{1,2,3,4*}

Inhibitor of apoptosis proteins (IAPs) maintain the balance between cell proliferation and cell death by inhibiting caspase activities and mediating immune responses. In the present study, a homolog of IAP (designated as *EslAP1*) was identified from Chinese mitten crab *Eriocheir sinensis*. *EslAP1* consisted of 451 amino acids containing two baculoviral IAP repeat (BIR) domains with the conserved Cx2 Cx6 Wx3 Dx5 Hx6 C motifs. *EslAP1* mRNA was expressed in various tissues and its expression level in hemocytes increased significantly ($p < 0.01$) at 12–48 h after lipopolysaccharide stimulation. In the hemocytes, *EslAP1* protein was mainly distributed in the cytoplasm. The hydrolytic activity of recombinant *EsCaspase-3/7-1* against the substrate Ac-DEVD-pNA decreased after incubation with *rEslAP1*. Moreover, *rEslAP1* could directly combine with *rEsCaspase-3/7-1* *in vitro*. After *EslAP1* was interfered by dsRNA, the mRNA expression and the hydrolytic activity of *EsCaspase-3/7-1* increased significantly, which was 2.26-fold ($p < 0.05$) and 1.71-fold ($p < 0.05$) compared to that in the dsGFP group, respectively. These results collectively demonstrated that *EslAP1* might play an important role in apoptosis pathway by regulating the activity of *EsCaspase-3/7-1* in *E. sinensis*.

Apoptosis is a type of cell death which plays an important role in regulating growth, development, and immune responses^{1,2}. Apoptosis is tightly controlled by multiple regulators, and the interaction between positive and negative regulators determines whether this program is activated or inhibited³. A family of cysteine-aspartic specific proteases known as caspases are considered as the executors of apoptosis, which cleave their substrates after the aspartate residue leading to protein degradation and apoptosis⁴. The modulation of apoptosis can be achieved by the dynamic expression of BCL-2 protein family members as well as the inhibitor of apoptosis proteins (IAPs)^{5,6}.

IAP was firstly recognized in baculoviruses which could inhibit apoptosis in infected cells in 1993⁷. Subsequently, numerous IAP homologues have been identified in vertebrates, which is primarily divided into five groups including X-linked IAP (XIAP), c-IAP1, c-IAP2, NAIP, and Survivin⁸. All the IAPs contain one to three baculovirus IAP repeats (BIR) domains, which is consisted of approximately 70 amino acid residues⁶. The IAP family members differ in the number of BIR domains, and some of them also contain a RING finger domain. XIAP, c-IAP1 and c-IAP2 comprise three BIRs in the N-terminus and a RING finger in the C-terminus, while NAIP contains three BIRs without RING finger domain, and Survivin and BRUCE include only one BIR⁹. Accumulating evidences have favored that some vertebrate IAPs, such as XIAP, c-IAP1 and c-IAP2, could directly bind to the activated caspase-3 and -7, and inhibit their activities^{10,11}. The BIR domains have been suggested to be responsible for the inhibition of caspases^{12,13}. For instance, the BIR motifs of c-IAP1 and c-IAP2 from *Homo sapiens* were evidenced for their ability to inhibit active recombinant caspases *in vitro*¹⁰. The BIR2 of XIAP from *H.*

¹Liaoning Key Laboratory of Marine Animal Immunology, Dalian Ocean University, Dalian, 116023, China.

²Laboratory of Marine Fisheries Science and Food Production Processes, Qingdao National Laboratory for Marine Science and Technology, Qingdao, 266235, China. ³Liaoning Key Laboratory of Marine Animal Immunology & Disease Control, Dalian Ocean University, Dalian, 116023, China. ⁴Dalian Key Laboratory of Aquatic Animal Disease Prevention and Control, Dalian Ocean University, Dalian, 116023, China. *email: lshsong@dloou.edu.cn

sapiens, but not the BIR1 or the BIR3, was able to interact with caspase-3 and -7 with an apparent inhibition¹⁴. It was reported that the RING finger domain in IAPs could coordinate two zinc atoms¹⁵. In *H. sapiens*, the RING finger domain of XIAP could act as an E3 ubiquitin ligase¹⁶. Moreover, it could also recruit E2 ubiquitin-conjugating enzymes and transfer ubiquitin to its target proteins bound to IAPs^{17–19}.

Recently, IAP homologues have also been discovered in various species of invertebrates. The invertebrate IAP homologues also contain one to three BIR domains, and some of them possess a RING finger domain. Some invertebrate IAPs were found to share the similar function with their homologues in vertebrates, which could play vital roles in the regulation of apoptosis and immune response against invading pathogens. For example, DIAP1 and DIAP2 were identified in fruit fly *Drosophila melanogaster* with two and three BIR domains, respectively^{20,21}. DIAP2 was able to regulate the expression of antimicrobial peptides (AMPs) in response to gram-negative bacterial infection through modulating the immune deficiency (IMD) pathway in *D. melanogaster*^{22,23}. *LvIAP1* with three BIR domains identified from shrimp *Litopenaeus vannamei* was reported to play vital roles in the regulation of shrimp hemocyte apoptosis response against white spot syndrome virus stimulation²⁴. Two IAPs (named as CgIAP1 and CgIAP2) containing two BIR domains were characterized in pacific oyster *Crassostrea gigas*, and they were found to be involved in regulating the apoptosis pathway and immune defense against bacterial infections^{25,26}. It has been demonstrated that some IAPs could inhibit the activation of caspases in invertebrates. DIAP1 could interact with caspase DRONC and interfere its activation in *D. melanogaster*²¹. The BIR2 domain of CgIAP2 could interact with the initiator caspase CgCaspase-2 to participate in apoptosis inhibition²⁵. The diverse caspase family members have also been discovered in various species of crustacean. For example, three caspases (*EsCaspase-3*, -7 and -8) were characterized in *E. sinensis* to play crucial roles in Cadmium-induced apoptosis²⁷, and two caspases (*EsCaspase-3/7-1* and *EsCaspase-3-like*) were involved in innate immune response under pathogen induced apoptosis^{28,29}. In shrimp *L. vannamei*, there were four caspases (*LvCaspase-2*, -3, -4 and -5) identified to play role in the host defense against white spot syndrome virus³⁰. Compared with vertebrate IAPs and caspases, the knowledge about the interaction modes of the large family of invertebrate IAPs and caspases as well as their involvements in apoptosis is still quite meagre.

E. sinensis is one of the important economic species, and the industry of *E. sinensis* aquaculture has been increasing rapidly in China³¹. With the development of aquaculture, various diseases caused by bacteria, viruses or other pathogenic organisms have frequently occurred in cultured *E. sinensis* and caused catastrophic losses³². Therefore, the better understanding of immune response mechanism is helpful for controlling the diseases and reducing economic losses. In crabs, hemocytes are found to play crucial roles in defending against pathogen invasion and they can be induced to apoptosis after pathogen stimulation³³. IAPs as inhibitors of apoptosis proteins play critical roles in inhibiting the cell apoptosis. In the present study, a novel IAP (designated as *EsIAP1*) was identified from Chinese mitten crab *E. sinensis* with the objectives (1) to investigate its mRNA distribution in tissues and its mRNA expression profile in response to immune stimulations, (2) to determine its subcellular localization in crab hemocytes, (3) to validate the interaction of *rEsIAP1* and *rEsCaspase-3/7-1* *in vitro*, as well as the potential regulation between *EsIAP1* and *EsCaspase-3/7-1* *in vivo*, hopefully to provide more information to understand the apoptosis regulation mechanism in crustaceans.

Results

The sequence characteristics and phylogeny of *EsIAP1*. A novel sequence of *EsIAP1* (GenBank accession numbers MF351747) was identified from *E. sinensis* genome database. The open reading frame of *EsIAP1* was of 1,356 bp, encoding a predicted polypeptide of 451 amino acids with calculated molecular weight of approximately 50 kDa. SMART analysis demonstrated that *EsIAP1* contained two BIR domains (BIR1 and BIR2). The conserved cysteine and histidine residues and the spacing between them in the reported BIR2 domains (Cx₂ Cx₆ Wx₃ Dx₅ Hx₆ C) were also identified in the BIR2 domain of *EsIAP1* (Fig. 1a). The deduced amino acid sequences of BIR1 and BIR2 domains of *EsIAP1* shared high sequence similarities with the corresponding domains of other IAPs, such as those from *L. vannamei* IAP1 (40.5% and 50.7%), *Mus musculus* XIAP (43.1% and 45.9%), *H. sapiens* c-IAP2 (45.8% and 53.4%), *H. sapiens* XIAP (41.7% and 47.3%), *M. musculus* c-IAP2 (44.4% and 49.3%), *D. melanogaster* DIAP2 (41.7% and 46.6%), *Bombyx mori* IAP (53.5% and 58.9%), *H. sapiens* c-IAP1 (43.1% and 50.7%), *M. musculus* c-IAP1 (43.1% and 50.7%), *C. gigas* (36.1% and 57.5%), and *Penaeus monodon* IAP (40.5% and 50.7%) (Fig. 1b). To evaluate the evolutionary relationship of *EsIAP1*, a phylogenetic tree was constructed based on the amino acid sequences of 13 IAP members by the neighbor-joining method. *EsIAP1* was firstly clustered with other arthropod IAPs in the phylogenetic tree, and then grouped with invertebrate IAPs, and finally clustered into the vertebrate XIAPs and c-IAPs (Fig. 1c).

Tissue distribution of *EsIAP1* mRNA and subcellular localization of *EsIAP1* in hemocytes. The mRNA transcripts of *EsIAP1* could be detected in all the examined tissues, including hemocytes, hepatopancreas, heart, gill, brain and muscle with the highest expression level in hepatopancreas, which was 5.24-fold ($p < 0.01$) of that in muscle. The expression level of *EsIAP1* mRNA in gill, hemocytes, heart and brain was 3.51-fold ($p < 0.01$), 3.41-fold ($p < 0.01$), 2.16-fold ($p < 0.05$) and 1.61-fold ($p > 0.05$) of that in muscle, respectively (Fig. 2a).

The purified *rEsIAP1* was employed to prepare polyclonal antibody (Fig. 2b, Supplementary Fig. S1). A clear band with 55 kDa was revealed by western blotting assay, indicating the high recognition specificity of the polyclonal antibody against *EsIAP1* (Fig. 2b, Supplementary Fig. S1). Pre-immune serum was used as negative control and no bands were detected (Fig. 2b, Supplementary Fig. S1). Western blotting assay of the native tissue sample with *EsIAP1* antibody revealed that there was a distinct band of 50 kDa (Fig. 2c). Immunofluorescence assay was performed to detect the localization of *EsIAP1* in hemocytes. The nucleus stained by DAPI was observed in blue, and the positive signal of *EsIAP1* was in green. The positive fluorescence signals were mainly observed in the cytoplasm of hemocytes according to the merged pictures (Fig. 2d).

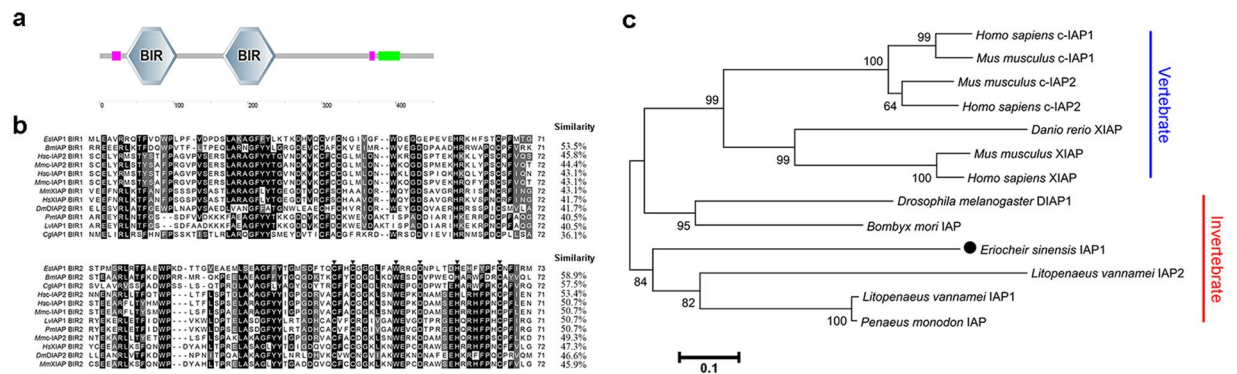


Figure 1. The sequence characteristics and phylogeny of *EsIAP1*. (a) The predicted structural domain of *EsIAP1*, which contains two BIR domains. (b) Multi-sequence alignment the amino acids sequences of BIR1 and BIR2 domains among IAP family members. The species and the GenBank accession numbers are as follows: *Homo sapiens* c-IAP1 (Q13490.2), *Mus musculus* c-IAP1 (Q62210.1), *H. sapiens* c-IAP2 (Q13489.2), *M. musculus* c-IAP2 (O08863.2), *M. musculus* XIAP (AAB58376.1), *H. sapiens* XIAP (AAC50373.1), *Litopenaeus vannamei* IAP1 (ADH03018.1), *Bombyx mori* IAP (NP_001037024), *Penaeus monodon* IAP (NP_001037024), *Crassostrea gigas* IAP1 (AEB54799.1), and *Drosophila melanogaster* DIAP2 (Q24307.3). Conserved cysteine and histidine residues of *EsIAP1* are marked with “▼”. Other conserved, but not consensus amino acids are shaded in gray. (c) The unrooted tree was built based on the amino acid sequences of 13 IAP family members. The species and the GenBank accession numbers were as follows: *H. sapiens* c-IAP1 (Q13490.2), *M. musculus* c-IAP1 (Q62210.1), *H. sapiens* c-IAP2 (Q13489.2), *M. musculus* c-IAP2 (O08863.2), *M. musculus* XIAP (AAB58376.1), *H. sapiens* XIAP (AAC50373.1), *L. vannamei* IAP1 (ADH03018.1), *L. vannamei* IAP2 (ADY38394.1), *P. monodon* IAP (ABO38431.1), *Danio rerio* XIAP (AAI33127.1), *B. mori* IAP (NP_001037024), *D. melanogaster* DIAP1 (Q24306.2) and *E. sinensis* IAP1 (AWK27045).

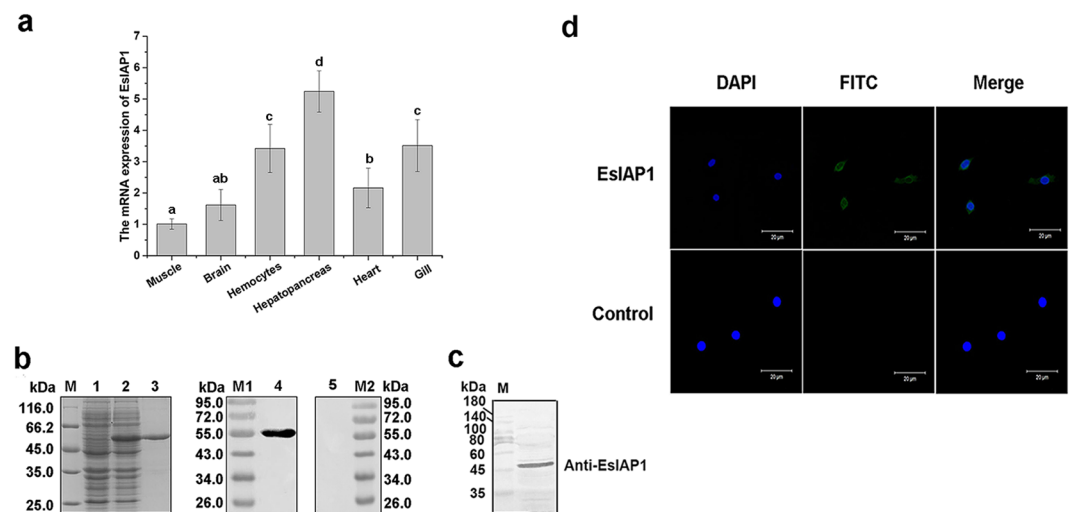


Figure 2. The mRNA expression of *EsIAP1* in crabs and subcellular localization of *EsIAP1* in hemocytes. (a) Quantitative real-time PCR (qRT-PCR) analysis of the expression level of *EsIAP1* mRNA in different tissues. The different letters show that there exist significant differences comparing with other groups ($p < 0.05$). (b) SDS-PAGE and western blotting analysis of r*EsIAP1*. Lane M: protein marker; Lane 1: negative control for r*EsIAP1* (without IPTG induction); Lane 2: IPTG induced r*EsIAP1*; Lane 3: purified r*EsIAP1*. Lane M1: protein marker; Lane 4: western blotting analysis of the r*EsIAP1*; Lane 5: western blotting analysis of the pre-immune serum from mice; Lane M2: protein marker. (c) The specific antibody detection of native *EsIAP1*. (d) Localization of *EsIAP1* in hemocytes. Immunohistochemistry was performed to analyze the expression of *EsIAP1* in hemocytes of *E. sinensis*. After incubation of polyclonal antibody of *EsIAP1* or pre-immune serum (negative control), Alexa Fluor 488-labeled goat-anti-mouse antibody was used to detect *EsIAP1*. Nucleus was stained with DAPI (blue). Positive signals of *EsIAP1* were shown in green. Scale bar = 20 μm . (For interpretation of the references to colour in this figure legend, the reader is referred to the web version of this article).

The expression of *EsIAP1* mRNA in hemocytes after LPS and *A. hydrophila* stimulations. The expression level of *EsIAP1* mRNA in hemocytes increased significantly after the stimulations with LPS and *A. hydrophila*. After LPS stimulation, the mRNA transcripts of *EsIAP1* increased significantly at 12 h (2.80-fold

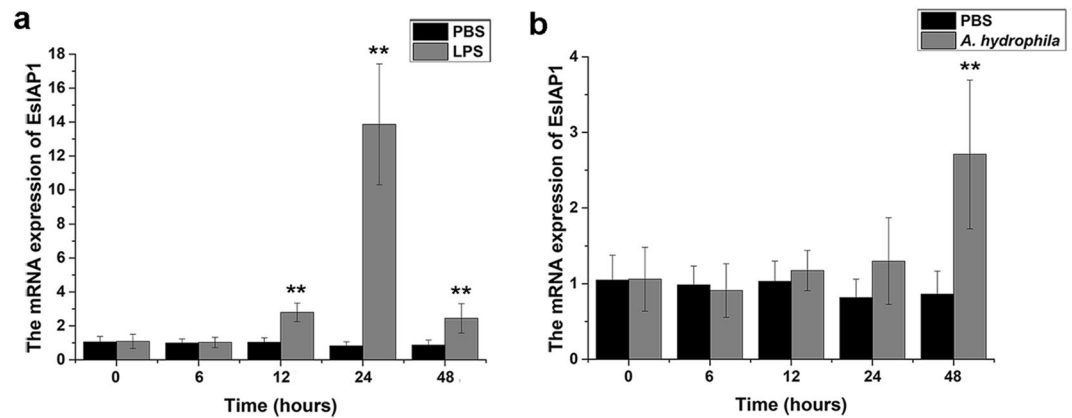


Figure 3. Temporal expression of the *EsIAP1* transcripts in hemocytes after LPS and *A. hydrophila* stimulations. **(a)** qRT-PCR detection of the expressions of *EsIAP1* in crabs challenged by LPS. **(b)** qRT-PCR detection of the expressions of *EsIAP1* in crabs challenged by *A. hydrophila*.

compared with that in PBS group, $p < 0.01$), reached the highest level of 13.86-fold ($p < 0.01$) at 24 h, and finally down-regulated to 2.44-fold ($p < 0.01$) at 48 h (Fig. 3a). After *A. hydrophila* stimulation, the relative expression level of *EsIAP1* mRNA kept at quite low level and there was no significant difference from 0 to 24 h compared with that in PBS group. However, it increased significantly (2.71-fold of control group, $p < 0.01$) at 48 h post *A. hydrophila* stimulation (Fig. 3b).

The mRNA expression of *EsCaspase-3/7-1* and the activity of caspases in hemocytes after the gene silencing of *EsIAP1*. To further explore the function of *EsIAP1* *in vivo*, the dsRNA-induced RNA interference (RNAi) was used to inhibit the expression of *EsIAP1*. The mRNA expression of *EsIAP1* in hemocytes decreased to 0.47-fold ($p < 0.05$) (Fig. 4a), while the mRNA expression of *EsCaspase-3/7-1* increased to 2.26-fold ($p < 0.05$) (Fig. 4b) at 24 h post the injection with sequence-specific dsRNA targeting *EsIAP1* compared to that in dsGFP group. After *EsIAP1* was silenced, the activity of caspase towards Ac-DEVD-pNA in hemocytes increased to 1.71-fold ($p < 0.05$) compared to that in the dsGFP group. While the activity of caspase-1 towards Ac-YAVD-pNA and caspase-6 towards Ac-VEID-pNA in hemocytes increased to 1.21-fold ($p > 0.05$) and 1.25-fold ($p > 0.05$) of that in the dsGFP group, respectively (Fig. 4c).

The interaction of r*EsIAP1* with r*EsCaspase-3/7-1* *in vitro*. The interaction of *EsIAP1* with *EsCaspase-3/7-1* was analyzed by pull down assay to understand the regulatory mechanism of apoptosis. The full-length ORFs of *EsIAP1* and *EsCaspase-3/7-1* were expressed, and the purified r*EsIAP1* and r*EsCaspase-3/7-1* (Fig. 5a-b, Supplementary Fig. S2a-b) were used for GST and His pull down assays. Two distinct bands were observed in the elute liquid after pull down assay (Fig. 5c-d, Supplementary Fig. S2c-d). The results indicated that r*EsIAP1* could directly combine and interact with r*EsCaspase-3/7-1* *in vitro*.

The hydrolytic activity of r*EsCaspase-3/7-1* after incubation with r*EsIAP1* *in vitro*. The hydrolyzing assay of caspase-3 substrate was employed to investigate the activity of r*EsIAP1*. The hydrolytic activity of r*EsCaspase-3/7-1* was significantly inhibited after the incubation with r*EsIAP1*. r*EsCaspase-3/7-1* displayed high hydrolytic activity towards Ac-DEVD-pNA (0.44 units per mg protein). After r*EsCaspase-3/7-1* was incubated with r*EsIAP1* or Z-VAD-FMK, the hydrolytic activities were 0.25 and 0.15 units per mg protein, respectively, which were significantly lower than that in r*EsCaspase-3/7-1* group ($p < 0.05$) (Fig. 5e).

Discussion

Apoptosis represents a fundamental biological process that relies on the activation of caspases³⁴. IAPs are a family of negative regulators of both caspases and cell death³⁵. In the present study, a novel IAP was identified from *E. sinensis* (designated *EsIAP1*). There were two BIR domains identified in *EsIAP1*, which was the typical domain of IAP family⁶. The deduced amino acid sequences of BIR1 and BIR2 domains in *EsIAP1* shared high similarities (36.1%~53.5% and 45.9%~58.9%, respectively) with the corresponding domains of other IAP proteins (Fig. 1a,b). Moreover, the conserved spacing of cysteine and histidine residues (Cx₂ Cx₆ Wx₃ Dx₅ Hx₆ C) in the other reported BIR2 domains were also found in *EsIAP1*, which was suggested to contribute to a novel zinc-binding fold⁶. These results suggested that *EsIAP1* was a typical IAP family member. In the phylogenetic tree, *EsIAP1* was firstly grouped with the crustacean IAPs to form a separated clade, then grouped with other arthropod IAP proteins, and finally clustered with vertebrate IAP proteins (Fig. 1c). These evidences collectively indicated that *EsIAP1* belonged to the IAP family in crustaceans.

As regulators of the apoptotic machinery, IAPs play important roles in many physiological processes, including homeostasis maintenance, development of tissues, and immune responses^{22,36,37}. In the present study, the mRNA transcripts of *EsIAP1* could be detected in all the examined tissues including hemocytes, hepatopancreas, gill, muscle, brain, and heart (Fig. 2a). Similarly, the transcripts of *CgIAP2* were also detected in various tissues in oyster *C. gigas*²⁵. The constitutive expression profile of *EsIAP1* indicated that it might involve in

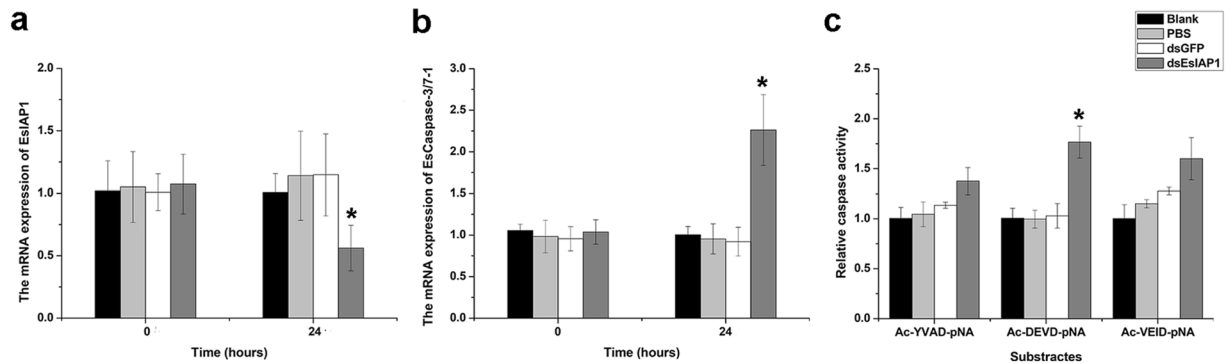


Figure 4. The mRNA and activity of caspase after the gene silencing of *EsIAP1*. (a) The expression level of *EsIAP1* mRNA in hemocytes after gene silencing of *EsIAP1*. Comparison of the level of *EsIAP1* was normalized to dsGFP group. (b) The expression level of the *EsCaspase-3/7-1* mRNA in hemocytes of *EsIAP1*-interfered crabs. Comparison of the level of *EsIAP1* was normalized to dsGFP group. (c) The activities of caspases were determined by measuring hydrolyzing activity against Ac-YVAD-pNA (substrate of caspase-1), Ac-DEVD-pNA (substrate of caspase-3) or Ac-VEID-pNA (substrate of caspase-6).

many physiological processes of crabs. It has been reported that IAPs could regulate the activity of caspases, further modulate cell cycle proliferation and receptor-mediated signal transduction⁹. The higher level of *EsIAP1* mRNA was observed in immune-associated tissues, including hemocytes, hepatopancreas and gill, which might be attributed to the cellular metabolism and innate immunity^{38,39}. Crustacean hemocytes play important roles in the host immune response, including recognition, phagocytosis and cell communication^{33,40,41}. Moreover, the high level of *EsCaspase-3/7-1* and *EsCaspase-3*-like were observed in hemocytes^{28,29}. The hemocytes were thus chosen as target to analyze the expression of *EsIAP1*. In the present study, the location of *EsIAP1* in hemocytes was observed by immunofluorescence assay, and the positive signal was found to be mainly distributed in the cytoplasm, which was similar as the previous reports in other species^{42–45}, possibly for the sake of binding to cytoplasmic caspase to regulate hemocyte apoptosis. LPS, a vital component of the outer wall of gram-negative bacteria, could trigger caspase-mediated apoptosis pathway^{42,46}. The apoptosis pathway is regulated by initiator caspases (such as caspase-8 and caspase-10), which can be triggered by death receptor (like Fas, TNFR1 and TRAIL-R1/R2) to initiate the activity of effector caspases^{43–45}. In the present study, the expression level of *EsIAP1* mRNA was significantly up-regulated after LPS and *A. hydrophila* stimulations (Fig. 3a,b). It has been reported that apoptosis pathway could be activated after LPS and *A. hydrophila* stimulations in crustacean^{47,48}. In *C. gigas*, *CgIAP2* was proposed to play a role in apoptosis inhibition in the immune defense against bacterial challenge²⁵. Some crustacean IAPs such as *PmIAP* and *LvIAP1* were suggested to be central to the regulation of hemocyte apoptosis^{24,49}. These results suggested that *EsIAP1* might exert important roles in immune defenses by regulating the apoptosis pathway in *E. sinensis*.

IAPs could regulate apoptosis through controlling caspase activities and caspase-activating platform formations, which also appeared to be important determinants of the responses of cells to endogenous or exogenous cellular injuries¹³. It was reported that c-IAP1 and c-IAP2 could directly bind to the activated caspase-3 and -7 to inhibit their activities in vertebrates¹⁰. In the present study, *EsCaspase-3/7-1*, an effector caspase, identified previously from *E. sinensis*²⁸, were employed to investigate the binding activity of *EsIAP1* with caspase. After *rEsCaspase-3/7-1* was incubated with *rEsIAP1* or Z-VAD-FMK, the hydrolyzing activity of *rEsCaspase-3/7-1* was significantly decreased (Fig. 5e). This result was in coincidence with the observation that IAPs could inhibit the activation of effector caspase^{13,20}. The direct combination of *rEsIAP1* with *rEsCaspase-3/7-1* confirmed by pull down assay might explain the decrease of *rEsCaspase-3/7-1* hydrolyzing activity after incubation with *rEsIAP1* *in vitro*. These results suggested that *rEsIAP1* could inhibit the hydrolytic activity of *rEsCaspase-3/7-1* by interacting with *rEsCaspase-3/7-1*. Furthermore, the expression of *EsCaspase-3/7-1* mRNA in hemocytes of crabs were significantly increased after the interference of *EsIAP1*, indicating the inhibitory regulation of *EsIAP1* on *EsCaspase-3/7-1*. The hydrolytic activity of caspase-3 was increased in hemocytes rather than caspase-1 and -6 after *EsIAP1* was silenced. These results showed that *EsIAP1* could regulate *EsCaspase-3/7-1* and further inhibit hemocyte apoptosis *in vivo*. Similarly, the number of circulating hemocytes was increased in *LvIAP1*-silenced shrimp because of the extensive apoptosis²⁴. Some mammalian IAPs, such as c-IAP1 and c-IAP2, were also found to be involved in signaling cascades, and play important roles in TNF-induced apoptosis⁵⁰. Therefore, it was speculated that *EsIAP1* could inhibit apoptosis by regulating *EsCaspase-3/7-1* in *E. sinensis*.

Caspases are activated to gain the full catalytic activity after being proteolytically cleaved to initiate apoptosis⁵¹. *EsCaspase-3*, -7 and -8 are characterized to play crucial roles in Cadmium-induced apoptosis²⁷, and *EsCaspase-3/7-1* and *EsCaspase-3*-like protein are found to be involved in innate immune response and induce apoptosis under pathogen stimulation^{28,29}. IAPs inhibit such proteolytically activated caspases, and further regulate apoptosis⁵². The loss or inhibition of cIAP1, cIAP2 and XIAP causes the majority of cells to be sensitized to death receptor to induce cell death⁵³. In *Drosophila*, DIAP1 normally inhibits both initiator and effector caspases^{54,55}. In summary, this study suggested that LPS and bacterial challenge could activate the apoptosis pathway in *E. sinensis*. *EsIAP1* could inhibit apoptosis by directly combining with *EsCaspase-3/7-1* and inhibit

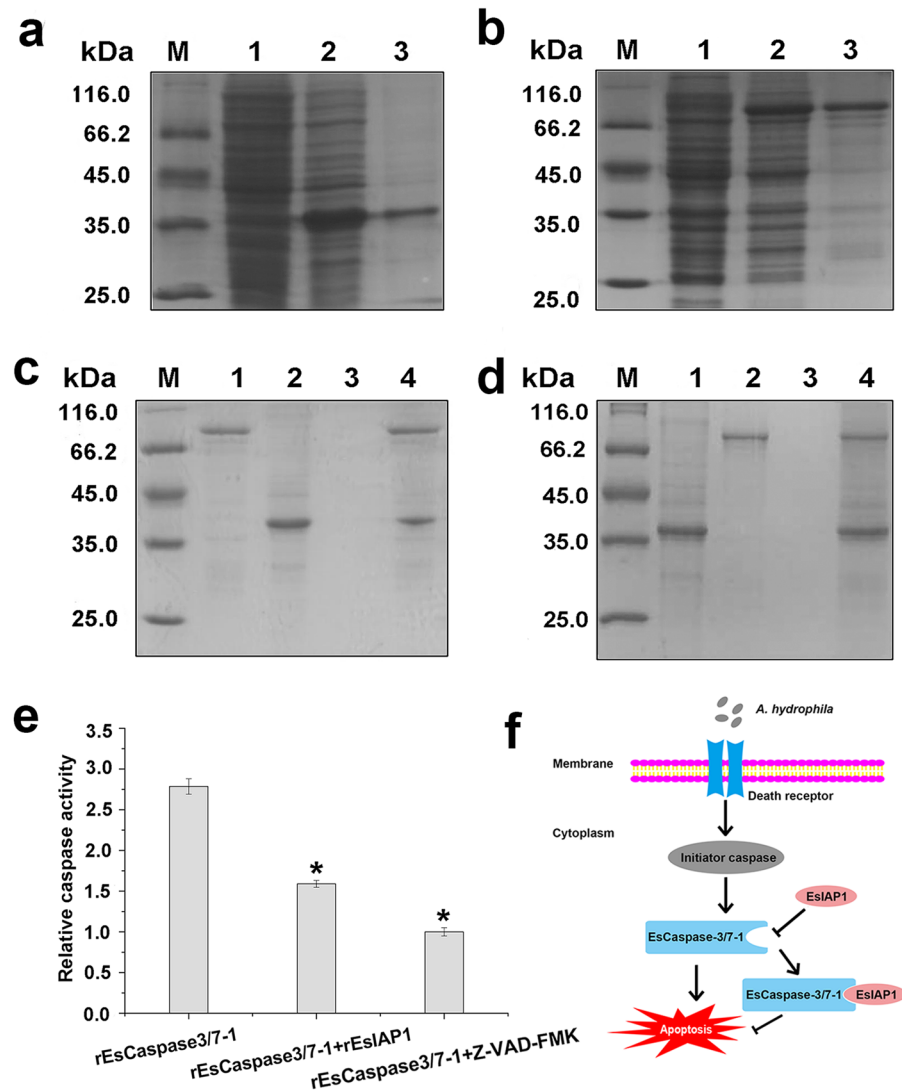


Figure 5. Interaction between *EsIAP1* and *EsCaspase-3/7-1* *in vitro*. (a) Purified r*EsCaspase-3/7-1* (His). Lane 1: negative control for r*EsCaspase-3/7-1* (His) (without IPTG induction); Lane 2: IPTG induced r*EsCaspase-3/7-1* (His); Lane 3: purified r*EsCaspase-3/7-1* (His). (b) Purified r*EsIAP1* (GST). Lane 1: negative control for r*EsIAP1* (GST, without IPTG induction); Lane 2: IPTG induced r*EsIAP1* (GST); Lane 3: purified r*EsIAP1* (GST). (c) Pull down by r*EsIAP1* (GST). Lane 1: purified r*EsIAP1* (GST); Lane 2: purified r*EsCaspase-3/7-1* (His); Lane 3: washed liquid; Lane 4: eluted liquid. (d) Pull down by r*EsCaspase-3/7-1* (His). Lane 1: purified r*EsCaspase-3/7-1* (His); Lane 2: purified r*EsIAP1* (GST); Lane 3: washed liquid; Lane 4: eluted liquid. (e) The activity of r*EsIAP1* was detected with caspase-3 activity assay kit. (f) Model for *EsIAP1* involvement in apoptosis pathway. *A. hydrophila* could activate caspase-mediated apoptosis pathway to initiate the activity of *EsCaspase-3/7-1* to lead to hemocyte apoptosis. *EsIAP1* could combine with *EsCaspase-3/7-1* to inhibit the hemocyte apoptosis.

its hydrolytic activity (Fig. 5f). These results provided novel idea to understand the modulatory role of IAP in apoptosis pathway in crustaceans.

Materials and Methods

Crabs, collection of tissues and immune stimulations. The crabs with an average weight of 20 g were collected from a commercial farm in Lianyungang, China, and cultured in aerated freshwater at $20 \pm 2^\circ\text{C}$ for one week before processing²⁸. Six crabs were sacrificed for determining the expression of *EsIAP1* mRNA in different tissues. The tissues including muscle, heart, brain, hepatopancreas and gill were collected from crabs to detect the mRNA expression of *EsIAP1* according to the previous study⁵⁶. The hemolymph drawing from the last pair of walking legs from each crab by using a syringe was mixed with anticoagulant solution (510 mM NaCl, 100 mM glucose, 200 mM citric acid, 30 mM sodium citrate, 10 mM EDTA-2Na, pH 7.3) at a ratio of 1:1, and the hemocytes were harvested by centrifugation⁵⁷. Tissues from two crabs were pooled together as one sample and there were three duplicates for each assay according to the previous methods⁵⁸. The crabs were treated by the injections

Primers	Sequence (5'-3')
<i>EsIAP1</i> -F	ATGGACATGTCTCGTCGGCAGTT
<i>EsIAP1</i> -R	TCAGCCGATGATGGGCCG
<i>rEsCaspase-3/7-1</i> -F	GGGAATTCATATGGATAACATCAAGGAAAATGG
<i>rEsCaspase-3/7-1</i> -R	CCGCTCGAGATACTTGGGAGACAGGAAGACCT
<i>rEsIAP1</i> -F (His)	GGAATTCATATGGACATGTCTCGGCAGTT
<i>rEsIAP1</i> -R (His)	CCGCTCGAGGCCGATGATGGGCCG
<i>rEsIAP1</i> -F(GST)	CGCGGATCCATGGACATGTCTCGGCAGTT
<i>EsIAP1</i> -R(GST)	ACGCGTCGACGCCGATGATGGGCCG
<i>EsIAP1</i> -RNAi-F	TAATACGACTCACTATAGGGATGGACATGTCTCGTCGGCAGTT
<i>EsIAP1</i> -RNAi-R	TAATACGACTCACTATAGGGGCCGATGATGGGCCG
GFP-RNAi-F	TAATACGACTCACTATAGGGCGACGTAACGGCCACAAGT
GFP-RNAi-R	TAATACGACTCACTATAGGGCTTGACAGCTCGTCCATGC
<i>EsIAP1</i> -qRT-F	CGCCAGGGTTTTCCAGTCACGAC
<i>EsIAP1</i> -qRT-R	CATCAAGGAGAACTGTGCT
<i>EsCaspase-3/7-1</i> -qRT-F	CCACCACTGCTGACTTCTTGATA
<i>EsCaspase-3/7-1</i> -qRT-R	AGACAGGAAGACCTTTCTCATCAA
<i>Es</i> - β -Actin-F	CCCATCTACGAGGGCTACGC
<i>Es</i> - β -Actin-R	CCTTGATGTCTCGCACGATTCT

Table 1. Primers used in this study.

of 100 μ L *Aeromonas hydrophila* (10^7 CFU mL⁻¹) and 100 μ L lipopolysaccharide (500 μ g mL⁻¹) according to the previous reports⁵⁹, respectively. Ninety crabs were employed and randomly divided into three groups. According to previous study, a volume of 100 μ L alive *A. hydrophila* (1×10^7 CFU mL⁻¹) or lipopolysaccharide (LPS from *Escherichia coli* 0111:B4, L2630, Sigma Aldrich, USA; 100 μ g mL⁻¹) resuspending in PBS (40 mM NaCl, 2.7 mM KCl, 10 mM Na₂HPO₄, 2 mM KH₂PO₄, pH 7.4) was injected into the arthrodial membrane of the last pair of walking legs in the stimulation groups, respectively^{28,59,60}. The crabs received an injection of 100 μ L PBS were employed as control group. Six crabs were randomly sampled from each group at 0, 6, 12, 24 and 48 h after treatments.

RNA extraction and cDNA synthesis. TRIzol reagent (Invitrogen) was used for the extraction of total RNA from *E. sinensis* tissue samples, and the first-strand cDNA was synthesised by using the PrimeScript™ real-time PCR kit (Takara, Japan) according to the manufacturer's instruction.

Sequence analysis of *EsIAP1*. The sequence of IAP genes was analyzed by BLASTP (<http://blast.ncbi.nlm.nih.gov/Blast.cgi>) in the genome database (PRJNA305216) of *E. sinensis*⁶¹. The primers (*EsIAP1*-F and -R) were designed to clone the open reading frame (ORF) of *EsIAP1*. The multiple sequence alignments were created by Clustal W. The conserved domain was identified through the SMART (<http://smart.embl-heidelberg.de/>). MEGA6.0 package was used to construct phylogenetic tree.

Purification of recombinant protein and preparation of polyclonal antibody. The full-length ORF sequences of *EsIAP1* and *EsCaspase-3/7-1* were amplified with specific primers (*rEsIAP1*-His-F and -R, *rEsCaspase-3/7-1*-F and -R) (Table 1). The PCR products were inserted into pET-22b vector (Novagen) with a His-tag. *rEsIAP1*-GST-F and -R (Table 1) were used to amplify *EsIAP1*, and the PCR products were inserted into the pGEX4T-1 vector (GE Healthcare) with a GST-tag. All those recombinant plasmids were transformed into *E. coli* BL21 (DE3) competent cells. These prokaryotic proteins were purified by a Ni²⁺ chelating sepharose column or GST-resin, following the manufacturers' instructions. Their concentrations were measured by BCA kit (Beyotime). The preparation of antiserum was performed as previously described⁶².

Western blotting and immunohistochemistry analysis of *EsIAP1*. The western blotting assay was performed according to the previous report²⁸. Recombinant protein was separated by SDS-PAGE, and transferred onto nitrocellulose membrane. After blocking for 1 h with 5% non-fat milk in TBST, the membrane was incubated successively with 1/1000 diluted poly-antibody of anti-*EsIAP1* as first antibody and 1/10,000 diluted goat-anti-mouse IgG (Sangon) as secondary antibody. After washing in TBST, the membrane dipped in ECL substrate system (Thermo Scientific) for 2 min, then imaged by Amersham Imager 600 (General Electric Company).

The hemocytes were resuspended with DMEM (Sangon) and then added into poly-L-lysine pre-coated dishes. After fixed with 4% paraformaldehyde (PFA, diluted in PBS), the dishes were blocked with 3% fetal bovine serum albumin (diluted in PBS) at 37 °C for 30 min, followed by washing with PBST (PBS with 0.1% tween-20). The dishes were then successively incubated with 1/1000 diluted anti-*EsIAP1* antibody at 37 °C for 1 h and 1/1,000 diluted Alexa Fluor 488-labeled goat-anti-mouse antibody at 37 °C for 1 h. After final washing with PBST, DAPI (1 μ g/mL in PBS) was used to stain the nucleus, and the dishes were observed by fluorescence microscope (ZEISS).

RNA interference. The RNA interference assay of *EsIAP1* was performed according to the previous report³². T7 promoter linked primers (GFP-RNAi-F and -R, *EsIAP1*-RNAi-F and -R) were used to amplify the cDNA sequence of dsGFP (657 bp) and ds*EsIAP1* (1,356 bp), respectively. The dsRNAs of *EsIAP1* and GFP were diluted

with PBS to the final concentration of $0.5 \mu\text{g} \mu\text{L}^{-1}$. The crabs were treated by the injections with $100 \mu\text{L}$ PBS, dsGFP and ds*EsIAP1*, respectively. The untreated crabs were used as blank group. Six crabs from each group were randomly sampled at 0 and 24 h post injections. The hemocytes were divided into two parts, and one aliquot of hemocyte sample was used to estimate the silencing efficiency, while the other was used for the measurement of caspase activity.

Quantitative real-time PCR (qRT-PCR) analysis of mRNA expression. qRT-PCR was conducted according to the previous reports⁶³. Two primers, *EsIAP1*-qRT-F and -R, were used in qRT-PCR to detect the expression of *EsIAP1*. The fragment amplified by primers of *Es*- β -actin (*Es*- β -Actin-F and -R) were employed as reference. The gene expression analysis was performed using the $2^{-\Delta\Delta C_t}$ method⁶³, and all data were given in terms of relative mRNA expression of mean \pm S.E. (N = 3).

Pull down assay. The pull down assay was carried out according to the previous report⁶³. The proteins of *rEsIAP1* (GST) and *rEscaspase-3/7-1* (His) ($30 \mu\text{g}$) were mixed with $20 \mu\text{L}$ of glutathione resin (for GST-tagged proteins) or charged nickel-nitrilotriacetic acid beads (for His-tagged proteins), respectively. The mixture (resin and binding proteins) was incubated at room temperature for 2 h with slight rotation, and then washed for three times by centrifuging at $500 \times g$ for 3 min to remove the unbound proteins. The tested protein (*rEscaspase-3/7-1*-His and *rEsIAP1*-GST), without GST tag or His tag, was added into the mixture containing the nickel-nitrilotriacetic acid beads or glutathione resin, and gently rotated at room temperature for 2 h. After washing three times, the mixture was analyzed by SDS-PAGE.

The hydrolyzing function assays of *rEsIAP1* in vitro. The potential inhibiting hydrolytic activity of *rEsIAP1* was detected using the caspase-3 activity assay kit (Beyotime) under the manufacturer's manual¹⁰. The protein concentration of purified *rEsIAP1*-His and *rEscaspase-3/7-1* was adjusted to 1 mg mL^{-1} . There were three experimental groups, including blank group (*rEscaspase-3/7-1*), *rEsIAP1* group (*rEsIAP1* + *rEscaspase-3/7-1*), and Z-VAD-FMK (pan caspase inhibitor) group (Z-VAD-FMK + *rEscaspase-3/7-1*). *rEscaspase-3/7-1* protein in *rEsIAP1* and Z-VAD-FMK groups were pre-incubated with *rEsIAP1* and Z-VAD-FMK at final concentrations of $100 \mu\text{g mL}^{-1}$ and $100 \mu\text{M}$, respectively⁶⁴. The mixtures were incubated at 37°C for 1 h and absorbance value was monitored at 405 nm by the SpectraMax 190 (Molecular Devices, Sunnyvale, CA, USA). The blank group (*rEscaspase-3/7-1*) was employed as the control, and the hydrolytic activity of *rEsIAP1* was determined by comparing the hydrolytic activity of *rEscaspase-3/7-1* against Ac-DEVD-pNA.

Hydrolyzing activity analysis of caspases in *EsIAP1*-interfered crabs. The hydrolyzing activity of caspases in hemocytes was examined according to the method described by previous study²⁹. The hydrolytic activity of the crab hemocyte protein was detected at 0 and 24 h after the injection of *EsIAP1*-dsRNA. The protein concentration of the supernatant was measured using the Bradford Protein Assay Kit (Beyotime) and adjusted to 1 mg mL^{-1} with lysate buffer. The hydrolytic activity of caspases was examined with the substrate Ac-YAVD-pNA, Ac-DEVD-pNA and Ac-VEID-pNA using the caspase-1, -3 and -6 activity assay kit (Beyotime, Shanghai, China) under the manufacturer's manual. The absorbance values of the reaction mixture was monitored at 405 nm using Spectra Max 190 (Molecular Devices, Sunnyvale, CA, USA). The different absorbance values represented the cleavage and release of pNA. The blank group was used as the reference.

Statistical analysis. The data (represented as mean \pm S.E., N = 3) were calculated by using the $2^{-\Delta\Delta C_t}$ method⁶⁵, and analyzed with *t*-test. Significant differences across controls were indicated with an asterisk at $p < 0.05$, and two asterisks at $p < 0.01$.

Received: 25 July 2019; Accepted: 19 December 2019;

Published online: 31 December 2019

References

1. Steller, H. Mechanisms and genes of cellular suicide. *Science* **267**, 1445–1449 (1995).
2. Kiss, T. Apoptosis and its functional significance in molluscs. *Apoptosis* **15**, 313–321 (2010).
3. Danial, N. N. & Korsmeyer, S. J. Cell death: critical control points. *Cell* **116**, 205–219 (2004).
4. Fan, T. J., Han, L. H., Cong, R. S. & Liang, J. Caspase family proteases and apoptosis. *Acta Bioch. Bioph. Sin.* **37**, 719–727 (2005).
5. Youle, R. J. & Strasser, A. The BCL-2 protein family: opposing activities that mediate cell death. *Nat. Rev. Mol. Cell Biol.* **9**, 47–59 (2008).
6. Deveraux, Q. L. & Reed, J. C. IAP family proteins-suppressors of apoptosis. *Genes Dev.* **13**, 239–252 (1999).
7. Crook, N. E., Clem, R. J. & Miller, L. K. An apoptosis-inhibiting baculovirus gene with a zinc finger-like motif. *J. Virol.* **67**, 2168–2174 (1993).
8. O'Riordan, M. X., Bauler, L. D., Scott, F. L. & Duckett, C. S. Inhibitor of apoptosis proteins in eukaryotic evolution and development: a model of thematic conservation. *Dev. Cell* **15**, 497–508 (2008).
9. Yang, Y. L. & Li, X. M. The IAP family: endogenous caspase inhibitors with multiple biological activities. *Cell Res.* **10**, 169–177 (2000).
10. Natalie, R., Deveraux, Q. L., Takahashi, R., Salvesen, G. S. & Reed, J. C. The c-IAP-1 and c-IAP-2 proteins are direct inhibitors of specific caspases. *EMBO J.* **23**, 6914–6925 (1997).
11. Deveraux, Q. L., Takahashi, R., Salvesen, G. S. & Reed, J. C. X-linked IAP is a direct inhibitor of cell-death proteases. *Nature* **388**, 300–304 (1997).
12. Tamm, I. *et al.* IAP-family protein Survivin inhibits caspase activity and apoptosis induced by Fas (CD95), Bax, Caspases, and anticancer drugs. *Cancer Res.* **58**, 5315–5120 (1998).
13. Berthelet, J. & Dubrez, L. Regulation of apoptosis by inhibitors of apoptosis (IAPs). *Cell* **2**, 163–187 (2013).
14. Takahashi, R. *et al.* A single BIR domain of XIAP sufficient for inhibiting caspases. *J. Biol. Chem.* **273**, 7787–7790 (1998).
15. Borden, K. L. RING domains: master builders of molecular scaffolds. *J. Mol. Biol.* **295**, 1103–1112 (2000).
16. Liston, P., Fong, W. G. & Korneluk, R. G. The inhibitors of apoptosis: there is more to life than Bcl2. *Oncogene* **22**, 8568–8580 (2003).

17. Shin, H. *et al.* The BIR domain of IAP-like protein 2 is conformationally unstable: implications for caspase inhibition. *Biochem. J.* **385**, 1–10 (2005).
18. Ditzel, M. & Meier, P. IAP degradation decisive blow or altruistic sacrifice. *Trends Cell Biol.* **12**, 449–542 (2002).
19. Vaux, D. L. & Silke, J. IAPs, RINGs and ubiquitylation. *Nat. Rev. Mol. Cell Biol.* **6**, 287–297 (2005).
20. Meier, P., Silke, J., Leever, S. J. & Evan, G. I. The Drosophila caspase DRONC is regulated by DIAP1. *EMBO J.* **19**, 598–611 (2000).
21. Muro, I., Hay, B. A. & Clem, R. J. The Drosophila DIAP1 protein is required to prevent accumulation of a continuously generated, processed form of the apical caspase DRONC. *J. Biol. Chem.* **277**, 49644–49650 (2002).
22. Gesellchen, V., Kuttenkeuler, D., Steckel, M., Pelte, N. & Boutros, M. An RNA interference screen identifies inhibitor of apoptosis protein 2 as a regulator of innate immune signalling in Drosophila. *EMBO Rep.* **6**, 979–984 (2005).
23. Kleino, A. *et al.* Inhibitor of apoptosis 2 and TAK1-binding protein are components of the Drosophila Imd pathway. *EMBO J.* **24**, 3423–3434 (2005).
24. Leu, J. H. *et al.* Litopenaeus vannamei inhibitor of apoptosis protein 1 (LvIAP1) is essential for shrimp survival. *Dev. Comp. Immunol.* **38**, 78–87 (2012).
25. Qu, T. *et al.* Characterization of an inhibitor of apoptosis protein in Crassostrea gigas clarifies its role in apoptosis and immune defense. *Dev. Comp. Immunol.* **51**, 74–78 (2015).
26. Zhang, L. L., Li, L. & Zhang, G. F. Gene discovery, comparative analysis and expression profile reveal the complexity of the Crassostrea gigas apoptosis system. *Dev. Comp. Immunol.* **35**, 603–610 (2011).
27. Xu, Y. R. & Yang, W. X. Role of three EsCaspases during spermatogenesis and Cadmium-induced apoptosis in Eriocheir sinensis. *Aging* **10**, 1146–1165 (2018).
28. Qu, C. *et al.* A novel effector caspase (Caspase-3/7-1) involved in the regulation of immune homeostasis in Chinese mitten crab Eriocheir sinensis. *Fish Shellfish Immunol.* **83**, 76–83 (2018).
29. Wu, M. H. *et al.* Caspase-mediated apoptosis in crustaceans: cloning and functional characterization of EsCaspase-3-like protein from Eriocheir sinensis. *Fish Shellfish Immunol.* **41**, 625–632 (2014).
30. Wang, P. H. *et al.* Analysis of expression, cellular localization, and function of three inhibitors of apoptosis (IAPs) from Litopenaeus vannamei during WSSV infection and in regulation of antimicrobial peptide genes (AMPs). *PLoS One* **8**, e72592 (2013).
31. Wang, J. *et al.* Genetic improvement and breeding practices for Chinese mitten crab, Eriocheir sinensis. *J. World Aquacult. Soc.* **49**, 292–301 (2018).
32. Dong, C. H. *et al.* The immune responses in Chinese mitten crab Eriocheir sinensis challenged with double-stranded RNA. *Fish Shellfish Immunol.* **26**, 438–442 (2009).
33. Johansson, M. W., Keyser, P., Sritunyalucksana, K. & Soderhall, K. Crustacean haemocytes and haematopoiesis. *Aquaculture* **191**, 45–52 (2000).
34. Obexer, P. & Ausserlechner, M. J. X-linked inhibitor of apoptosis protein—a critical death resistance regulator and therapeutic target for personalized cancer therapy. *Front. Oncol.* **4**, 197 (2014).
35. Scott, F. L. *et al.* XIAP inhibits caspase-3 and -7 using two binding sites: evolutionarily conserved mechanism of IAPs. *EMBO J.* **24**, 645–655 (2005).
36. Xing, Z., Conway, E. M., Kang, C. & Winoto, A. Essential role of survivin, an inhibitor of apoptosis protein, in T cell development, maturation, and homeostasis. *J. Exp. Med.* **199**, 69–80 (2004).
37. Cai, Q. *et al.* A potent and orally active antagonist (SM-406/AT-406) of multiple inhibitor of apoptosis proteins (IAPs) in clinical development for cancer treatment. *J. Med. Chem.* **54**, 2714–2726 (2011).
38. Lavine, M. D. & Strand, M. R. Insect hemocytes and their role in immunity. *Insect Biochem. Molec.* **32**, 1295–1309 (2002).
39. Zhao, Z. Y. *et al.* Profiling of differentially expressed genes in hepatopancreas of white spot syndrome virus-resistant shrimp (Litopenaeus vannamei) by suppression subtractive hybridisation. *Fish Shellfish Immunol.* **22**, 520–534 (2007).
40. Bachere, E. *et al.* Knowledge and research prospects in marine mollusc and crustacean immunology. *Aquaculture* **132**, 17–32 (1995).
41. Adachi, K., Hirata, T., Nishioka, T. & Sakaguchi, M. Hemocyte components in crustaceans convert hemocyanin into a phenoloxidase-like enzyme. *Comp. Biochem. Physiol. B. Biochem. Mol. Biol.* **134**, 135–141 (2003).
42. Choi, K. B. *et al.* Lipopolysaccharide mediates endothelial apoptosis by a FADD-dependent pathway. *J. Biol. Chem.* **273**, 20185–20188 (1998).
43. Ye, J. *et al.* Protective effect of SIRT1 on toxicity of microglial-derived factors induced by LPS to PC12 cells via the p53-caspase-3-dependent apoptotic pathway. *Neurosci. Lett.* **553**, 72–77 (2013).
44. Ding, X. M. & Ding, W. X. Death receptor activation-induced hepatocyte apoptosis and liver injury. *Curr. Mol. Med.* **6**, 491–508 (2003).
45. Elmore, S. Apoptosis: a review of programmed cell death. *Toxicol. Pathol.* **35**, 495–516 (2007).
46. Cohen, G. M. Caspases: the executioners of apoptosis. *Biochem. J.* **326**, 1–16 (1997).
47. Xian, J. A., Miao, Y. T., Li, B., Guo, H. & Wang, A. L. Apoptosis of tiger shrimp (Penaeus monodon) haemocytes induced by Escherichia coli lipopolysaccharide. *Comp. Biochem. Physiol. A. Mol. Integr. Physiol.* **164**, 301–306 (2013).
48. Xu, H. S. *et al.* Effect of lipopolysaccharide on the hemocyte apoptosis of Eriocheir sinensis. *J. Zhejiang Univ. Sci. B.* **16**, 971–979 (2015).
49. Leu, J. H., Kuo, Y. C., Kou, G. H. & Lo, C. F. Molecular cloning and characterization of an inhibitor of apoptosis protein (IAP) from the tiger shrimp, Penaeus monodon. *Dev. Comp. Immunol.* **32**, 121–133 (2008).
50. Varfolomeev, E. *et al.* IAP antagonists induce autoubiquitination of c-IAPs, NF-kappaB activation, and TNFalpha-dependent apoptosis. *Cell* **131**, 669–681 (2007).
51. Vasudevan, D. & Ryoo, H. Regulation of cell death by IAPs and their antagonists. *Curr. Top. Dev. Biol.* **114**, 185–208 (2015).
52. Shapiro, P. J., Hsu, H. H., Jung, H., Robbins, E. S. & Ryoo, H. D. Regulation of the Drosophila apoptosome through feedback inhibition. *Nat. Cell Biol.* **10**, 1440–1446 (2008).
53. Vasilikos, L., Spilgies, L. M., Knop, J. & Wong, W. W. Regulating the balance between necroptosis, apoptosis and inflammation by inhibitors of apoptosis proteins. *Immunol. Cell Biol.* **95**, 160–165 (2017).
54. Tenev, T. *et al.* The Ripoptosome, a signaling platform that assembles in response to genotoxic stress and loss of IAPs. *Mol. Cell* **43**, 432–448 (2011).
55. Yan, N., Wu, J. W., Chai, J., Li, W. & Shi, Y. Molecular mechanisms of DrICE inhibition by DIAP1 and removal of inhibition by Reaper, Hid and Grim. *Nat. Struct. Mol. Biol.* **11**, 420–428 (2004).
56. Yang, W. *et al.* Beclin-1 is involved in the regulation of antimicrobial peptides expression in Chinese mitten crab Eriocheir sinensis. *Fish Shellfish Immunol.* **89**, 207–216 (2019).
57. Yang, W. *et al.* A novel nuclear factor Akirin regulating the expression of antimicrobial peptides in Chinese mitten crab Eriocheir sinensis. *Dev. Comp. Immunol.* **101**, 103451 (2019).
58. Qu, C. *et al.* The involvement of suppressor of cytokine signaling 6 (SOCS6) in immune response of Chinese mitten crab Eriocheir sinensis. *Fish Shellfish Immunol.* **72**, 502–509 (2018).
59. Jin, X. K. *et al.* Two novel short C-type lectin from Chinese mitten crab, Eriocheir sinensis, are induced in response to LPS challenged. *Fish Shellfish Immunol.* **33**, 1149–1158 (2012).
60. Jia, Z. H., Wang, M. Q., Wang, X. D., Wang, L. L. & Song, L. S. The receptor for activated C kinase 1 (RACK1) functions in hematopoiesis through JNK activation in Chinese mitten crab Eriocheir sinensis. *Fish Shellfish Immunol.* **57**, 252–261 (2016).
61. Song, L. S. *et al.* Draft genome of the Chinese mitten crab, Eriocheir sinensis. *Gigascience* **5**, 5 (2016).

62. Cheng, S. F., Zhan, W. B., Xing, J. & Sheng, X. Z. Development and characterization of monoclonal antibody to the lymphocystis disease virus of Japanese flounder *Paralichthys olivaceus* isolated from China. *J. Virol. Methods* **135**, 173–180 (2006).
63. Sun, J. J. *et al.* beta-Arrestins negatively regulate the Toll pathway in shrimp by preventing dorsal translocation and inhibiting Dorsal transcriptional activity. *J. Biol. Chem.* **291**, 7488–7504 (2016).
64. Xu, J. C. *et al.* Caspase-3 serves as an intracellular immune receptor specific for lipopolysaccharide in oyster *Crassostrea gigas*. *Dev. Comp. Immunol.* **61**, 1–12 (2016).
65. Livak, K. J. & Schmittgen, T. D. Analysis of relative gene expression data using Real-Time quantitative PCR and the $2^{-\Delta\Delta CT}$ method. *Methods* **25**, 402–408 (2001).

Acknowledgements

We are grateful to all the laboratory members for their technical advice and helpful discussions. We also thank Jiong Chen for helpful suggestions. This research was supported by National Key R&D Program (2018YFD0900606), NSFC (No. 31530069), AoShan Talents Cultivation Program Supported by Qingdao National Laboratory for Marine Science and Technology (No. 2017ASTCP-OS13), Dalian High Level Talent Innovation Support Program (2015R020), Program for Innovative Talents in Higher Education of Liaoning Province (LR2016036), the Research Foundation for Distinguished Professor in Liaoning (to L. S.) and Talented Scholars in Dalian Ocean University (to L. W.).

Author contributions

C.Q. prepared the experiments and figures. Experiments were assisted by J.-J.S., Q.-S. X., X.-J.L., W.Y., F.-F.W., Y.W., Q.-L.Y., Z.-H.J., L.-L.W. and L.-S.S. supervised the work. The manuscript was written by C.Q., J.-J.S. and edited by L.-S.S.

Competing interests

The authors declare no competing interests.

Additional information

Supplementary information is available for this paper at <https://doi.org/10.1038/s41598-019-56971-1>.

Correspondence and requests for materials should be addressed to L.S.

Reprints and permissions information is available at www.nature.com/reprints.

Publisher's note Springer Nature remains neutral with regard to jurisdictional claims in published maps and institutional affiliations.



Open Access This article is licensed under a Creative Commons Attribution 4.0 International License, which permits use, sharing, adaptation, distribution and reproduction in any medium or format, as long as you give appropriate credit to the original author(s) and the source, provide a link to the Creative Commons license, and indicate if changes were made. The images or other third party material in this article are included in the article's Creative Commons license, unless indicated otherwise in a credit line to the material. If material is not included in the article's Creative Commons license and your intended use is not permitted by statutory regulation or exceeds the permitted use, you will need to obtain permission directly from the copyright holder. To view a copy of this license, visit <http://creativecommons.org/licenses/by/4.0/>.

© The Author(s) 2019